Dynamic Modelling of Vehicle Collisions using the Finite Element Method. Cauchy Problem

Stanimir Karapetkov, Hristo Uzunov, Silvia Dechkova* and Vasil Uzunov

Technical University of Sofia, Faculty and College – Sliven, Bulgaria

_____

Abstract

This article discusses a boundary-value problem of impact between two cars, known as the Cauchy problem. The purpose of the task is to determine the two vehicles' center of mass velocity of motion prior impact, knowing the final rest positions after the accident and the crumple zone. Geometric modelling is performed in SolidWorks, and dynamic finite element analysis is carried out with Abaqus /Explicit. The initial data are the deformations of the vehicles in three-dimensional space and the respective boundary conditions. The movement of cars after the impact is modelled using a multi-mass spatial model. The macro movement is in a three-dimensional Cartesian coordinate system with six degrees of freedom. The deformation energy is determined by the finite element method for an elastoplastic body. The findings of the investigation are the initial conditions of macro movement of bodies after impact. The coincidence of the coordinates of the final rest positions of the cars and their trajectories on the previously described treds are an indicator of the reliability of the study. An example is given, based on real data driven from two car collision.

Keywords: traffic accident, two car collision, finite element model, engineering expert analysis, SolidWorks, Abaqus
_____

1. Introduction

Statistical analysis police reports show that the most serious vehicle collisions mainly constitute of two-car accidents. The proportion of this type of motor vehicle crash is the highest compared to the total percentage of events. Collisions between two cars occur in three interconnected phases. The first phase is the vehicle motion prior to impact in which they most often move in retarded motion until the impact. In this phase, external forces act on each of the cars, caused by the driver's reaction on the control and monitoring systems. The second phase is the impact phase, in which cars contact, deform and move. In this phase part of kinetic energy is absorbed, which is transformed into energy of deformation. The third phase includes post-impact motion of vehicles to a certain final rest position, which is a result of the available residual kinetic energy. This phase is known as the macro movement phase. Such movement is evident in case of complete loss of control to final rest position (Karapetkov, Dimitrov, Uzunov, Dechkova [1, 2], Zlatev, Ivanov [3], Niehoff, Gabler [4], Wach [5]).

Characteristic feature of this type of events is that in the impact phase there is actually a system of parallel forces, which are equated the same. The study of the impact phase is according to two basic rules:

The impulse-momentum change theorem has the form of

$$m.\vec{u} - m.\vec{V} = \vec{S} \qquad (1)$$

where m is total vehicle mass; $\vec{u}$ – velocity of the vehicle center of mass post collision; $\vec{V}$ –velocity of the vehicle center of mass prior collision; $\vec{S}$ – crash impulse.

The momentum change theorem applied to the vehicle mechanical system with respect to its mass center during its relative motion around it $d\vec{K}_C^r$ has the form of

$$\frac{d\vec{K}_C^r}{dt} = \vec{M}_C^{(e)} \qquad (2)$$

where $\vec{M}_C^{(e)}$ is the principle of moments of impact forces relative to the vehicle center of mass.

In reality, in the impact phase, from the initial moment of contact to the complete separation of the cars due to their displacement, the impact force system changes direction. Integrating the finite element method in a specifically designed model allows for the deformations of each car to be monitored, the shape and depth of indentation to be compared and the direction of the equivalent of the impact forces in the impact phase to be analysed.

2. Creating the dynamic model of two cars in collision

For the construction of the 3-D model cars, necessary for the impact process to be studied by the finite element method, the technical characteristics of real life vehicles in a real road accident were used. Geometric modelling was performed in SolidWorks (SolidWorks Simulation 2009 [6, 7], Dechkova [8]), and real research and dynamic analysis was carried out in Abaqus. The respective movable and immovable nodes between them were defined. For each detail, in addition to its geometric dimensions, the characteristics of the materials from which they had been made were also indicated. Based on these input data, the mass characteristics of the modelled object were determined. The created models in SolidWorks were imported into the Abaqus dynamic analysis software system (Nushtayev [9], Yehia [10]). The Abaqus/CAE system exported a sketch in the standard STEP file format, recording in it all the geometric data of the model layer.

Finite element modelling and computational procedures is a nonlinear dynamic analysis and is used to analyse the impact efficiency between the vehicles. The applied simulation covers a number of specific problems, which could be of the following kind:

The choice of mesh and type of element had to be carefully selected, especially in the area of contact between the two vehicles, in order to obtain accurate results regarding shape deformation. It should be as similar as possible to the one actually observed from first-hand inspection in the field accident.

About 7000 elements were generated for the whole model. The supposition was to use the smallest size of elements, of about 0.01 m, for the front contact area (bumber - radiators - hood and front doors). This completely determined the possibility of achieving identity of the deformed areas.

The Abaqus/Explicit package allows the study of elastic systems whose elements perform mutual movements. It is based on an unambiguously formulated differential equation (Žmindáka, Pelagića, Pastoreka, Močilana, Vybošťoka [11], Duni, Monfrino, Saponaro, Caudano, Urbinati [12]).

The differential equation of finite elements has the form of:

$$M\ddot{U} + C\dot{U} + KU = R(t) \tag{3}$$

where M is global mass; C - attenuation coefficient; K - stiffness matrix; R is the vector of external loads; $U,\ \dot{U},\ \ddot{U}$ - displacement, velocity and acceleration of a set of finite elements at the moment t.

The solution of the differential equation is of the form:

$$\ddot{U}(t) = \frac{R(t)^{(ext)} - R(t)^{(int)}}{M} \tag{4}$$

$R(t)^{(ext)}$ is the vector of external forces and $R(t)^{(int)}$ is a vector of internal forces.

Attenuation stability condition is determined by the expression

$$\Delta t \le \frac{2}{\omega_{max}}\left(\sqrt{1 + \xi_{max}^2} - \xi_{max}\right) \tag{5}$$

where ω_{max} is maximum natural circular frequency; ξ_{max} is the fraction of the critical attenuation in the highest mode. The introduction of a damper to the solution reduces the steady increase in time.

3. Dynamic modelling investigation of two car collisions

A collision between two cars Audi Q7 and Honda Civic in the area of an intersection has been investigated (Table 1). The area of mutual contact between them and the final rest position were known. During the impact and during the transition to final rest position the cars leave characteristic treds of friction of the car tires on the road surface. Their geometric arrangement is also known. A diagram of the real car crash is shown in Figure 1.
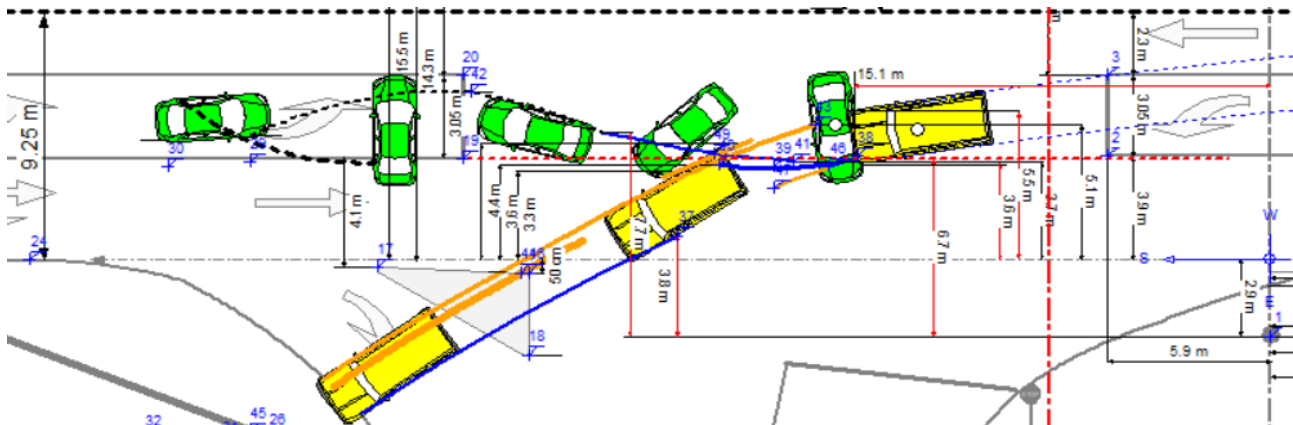

Fig. 1. Diagram of two car collision, real road accident. The event data are known from a video recorder, which identifies the point of contact, the trajectories of motion to the final rest position. They are shown in photos 1-4, taken by surveillance camera.

Photo 1   Photo 2   Photo 3   Photo 4

Table 1. Geometric dimensions, masses and mass moment of inertia of the two automobiles Audi and Honda, respectively.

	Audi	Honda
Total mass of the automobiles	2480 kg	1100 kg
Mass moment of inertia J_z	4960 kg m²	1650 kg m²

Length	5086 mm	4190 mm
Width	1983 mm	1695 mm
Height	1737 mm	1375 mm
Wheelbase	3002 mm	2620 mm
Front tred	1651 mm	1478 mm
Rear tred	1676 mm	1488 mm
Front drag coefficient	0,37	0,34
Drive	4x4	fore
Size tyres	235/60R18	185/70R14

4. Finite element model in Abaqus

A real model of impact between two finite element cars was created using the Abaqus/Explicit software (Fig. 2). In the automobile finite element models, second-order integration elements were used, as they use a lower mesh density than the first-order elements. The tetrahedral element of the second row has ten nodes (four angular and six internal) and each of them has three degrees of freedom. The edges and surfaces of the elements of the second row take curvilinear shapes after deformation. This justifies the chosen modelling approach, namely by applying the methods and means of curvilinear geometry.

Due to better ability to deploy and compose a second-order displacement field, second-order tetrahedral elements were used for multiple analyses in Abaqus/Explicit, although their calculation is more complex than that of first-order integration elements.

The degrees of freedom of a node in a network with a finite number of elements determine the ability of the node to perform translations. The number of degrees of freedom that a node has depends on the type of element to which the node belongs.

Meshing is a crucial stage in the analysis. The Abaqus/Explicit automated tool creates a mesh based on the dimensional size of the element. The system establishes this parameter, taking into account its volume and lateral surface area.
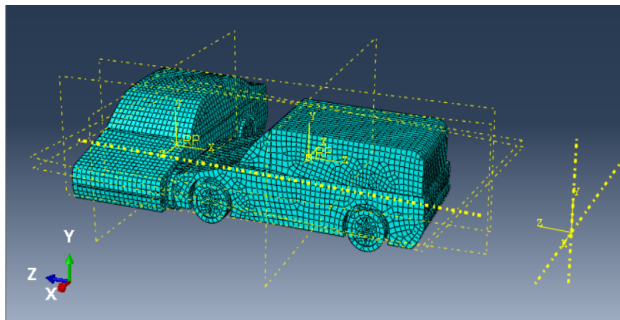

Fig. 2. Audi and Honda automobile model of finite elements in Abaqus.

5. Dynamic model in Abaqus/Explicit

Figure 3 shows a three-dimensional model consisting of two automobiles, an Audi and a Honda. A fixed coordinate system Z, X, Y is set, as well as the coordinate systems of z_{c1}, x_{c1}, y_{c1} and z_{c2}, x_{c2}, y_{c2}, which are invariably connected to the center of mass of each vehicle. The created 3D models are positioned on the basis of a selected fixed Cartesian coordinate system with a common point of the coordinates z_C and x_C.

Materials and their characteristics are selected from the Abaqus database. When choosing material, it is assumed that deformation depends linearly on strain. For this reason, the selected isotropic steel material Steel-30XGSA is considered

to be suitable. It has plasticity region characterized by the fact that significant deformations are accompanied by small changes in strain. The created car models have material density of $355 \, N/mm^2$ with isotropic hardening to a strength of $490 \, N/mm^2$ at plastic stress strain of 0.025.

It has been assumed that cars as solids will not introduce inaccuracies in obtaining initial results. The automobiles were modelled with standard body elements (Abaqus elements S3R and S4R) with thickness of 0.01 mm.
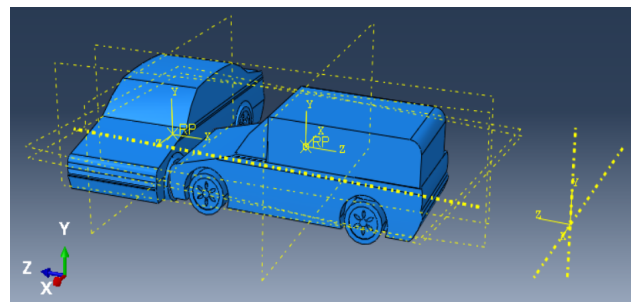

Fig. 3. Spatial model of Audi and Honda cars in Abaqus. The selected contact conditions between tires and ground allow for registration of friction between separate parts to be taken into account during their deformation. In this case, a coefficient of friction μ = 0.05 is set.

Loads are applied with the help of the so-called steps. For nonlinear problems, each load step consists of several iterations. Each load step can also have its own type of analysis, boundary conditions and output. In this case a step with 21 iterations was set.

The next step in the analysis is to set the boundary problem conditions and load the mechanical system. The boundary condition was defined by fixing certain surfaces of the cars.

Load was created by using volumetric gravitational forces - type Gravity (the self weight is taken into account). This type of load defines magnitude of self weight forces, calculated by Abaqus for each individual element considering the density of the material as well.

The initial conditions of the study were realized at the following kinematic parameters:

Audi car	Honda car
$\dot{z}_{11} = 85{,}9 \, km/h$	$\dot{z}_{21} = -2{,}6 \, km/h$
$\dot{x}_{11} = 13{,}6 \, km/h$	$\dot{x}_{21} = 18{,}7 \, km/h$
$\dot{\varphi}_{y11} = 0 \, s^{-1}$	$\dot{\varphi}_{y21} = 0 \, s^{-1}$

6. Findings of the dynamic analysis in Abaqus

The simulation in the dynamic model is performed using Abaqus/Explicit code. Dynamic analyses have been made, allowing visualization and tabular systematization of the results of the created model. The deformation analysis visualizes the displacements of the nodes along the three

coordinate axes "Magnitude" of impact between Audi and Honda cars (Fig. 4).

The final rest position of the cars corresponds to the following kinematic parameters:

Audi	Honda
$z_{12} = 23,7\ m$	$z_{22} = 30,6\ m$
$x_{12} = 7,7\ m$	$x_{22} = -1,5\ m$
$\varphi_{y12} = 35^o$	$\varphi_{y22} = 184^o$

Audi	Honda
$z_{11} = 6,01\ m$	$z_{21} = 9,1\ m$
$x_{11} = -0,69\ m$	$x_{21} = -1,73\ m$
$\varphi_{y11} = 9^o$	$\varphi_{y21} = 63^o$
$\dot{z}_{12} = 57\ km/h$	$\dot{z}_{22} = 59\ km/h$
$\dot{x}_{12} = 15\ km/h$	$\dot{x}_{22} = 3,1\ km/h$
$\dot{\varphi}_{y12} = 1,57\ s^{-1}$	$\dot{\varphi}_{y22} = -3,42\ s^{-1}$

Based on the dynamic investigation using the finite element method, the initial values of the macro-movement of the cars after impact are obtained:
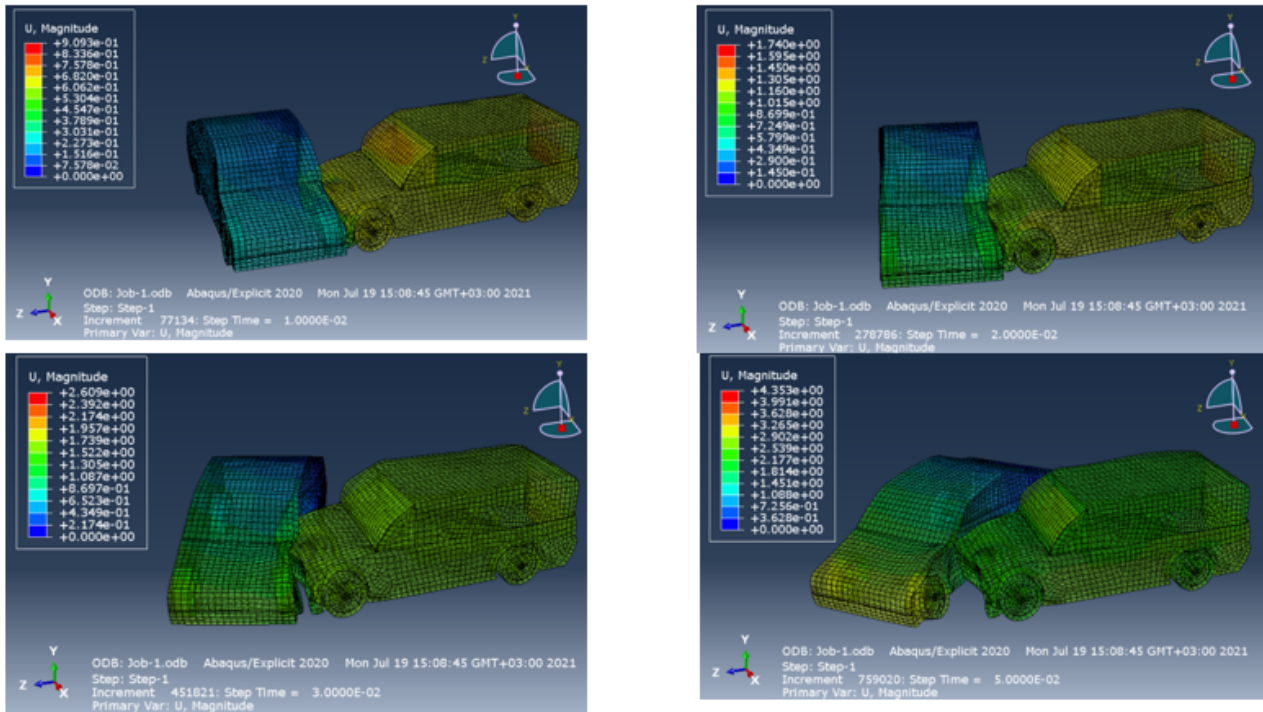
Fig. 4. Impact deformation between Audi and Honda in the time interval of $t = 0 \div 0.05\ s$.

The mean values form a function of the form y = f (x). An approximate function in the form of a Lagrange polynomial is sought:

$$P_n(x) = a_o + a_1.x + a_2.x^2 + \cdots + a_n.x^n$$

so that

$$P_n(x_i) = y_i, i = 0,1, \ldots, n.$$

The existence of such a polynomial is ensured by the following Lagrange interpolation polynomial, which has the form:

$$L_n(x) = \sum_{i=0}^{n} y_i . \prod_{\substack{j=0 \\ j \neq i}}^{n} \frac{(x - x_j)}{(x_i - x_j)} \qquad (6)$$

The results of the change of the specific kinematic parameters in the form of a polynomial and graphical dependence are shown in Figures 5 to 16.

The obtained values of the kinematic quantities in the final phase of the impact are the initial values of the macro movement of the cars after the impact.

Macro simulation of vehicle motion in case of loss of lateral stability is observed in an arbitrarily accepted absolute coordinate system $OXYZ$ (Sharma, Brophy [13], Neptune, Flynn [14], Campbell [15], Prasad [16], Prochowski, Żuchowski [17]). To study the car motion, it has been assumed that its own coordinate system $Cx'y'z'$ is movable and permenantly connected to the vehicle center of mass C (Fig. 17). In addition, a permanently connected $Cxyz$ coordinate system is attached to it, parallel to the absolute and translationally movable one. Coordinates of the vehicle center of mass C x_c, y_c, z_c in the fixed coordinate system are selected for generalized coordinates of the car motion.

Rotational motion of the car is expressed by the Euler transformations and corresponding angles, namely ψ, θ and φ. The precession angle of ψ, taking into account the rotation around the axis Cz; respectively, the angular velocity of $\dot{\psi}$ is obtained; the angle θ of nutation, taking into account the rotation with respect to the axis C_ρ, the intersection of the planes Oxy and $Cx'y$.
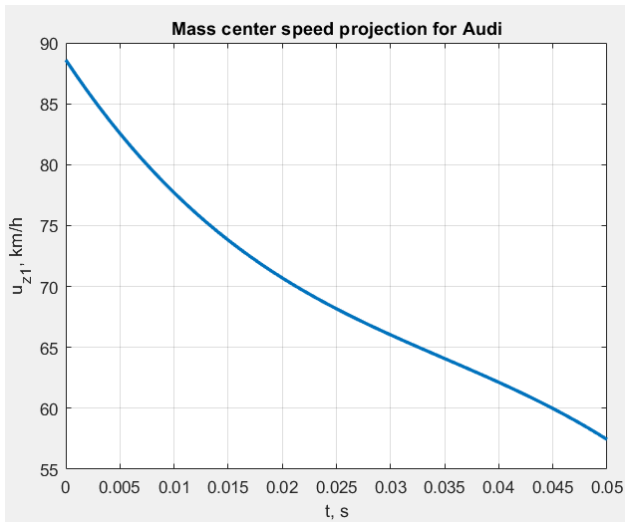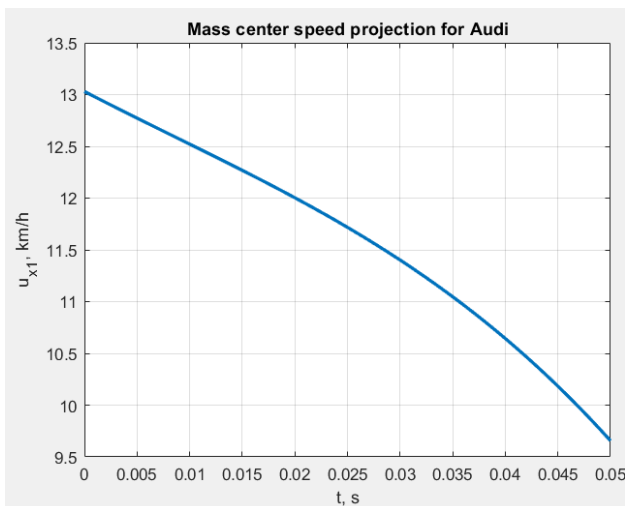
$$\dot{z}_1 = -2{,}607.10^5.t^3 + +2{,}731.10^4.t^2 - 1337.t + 88{,}6$$

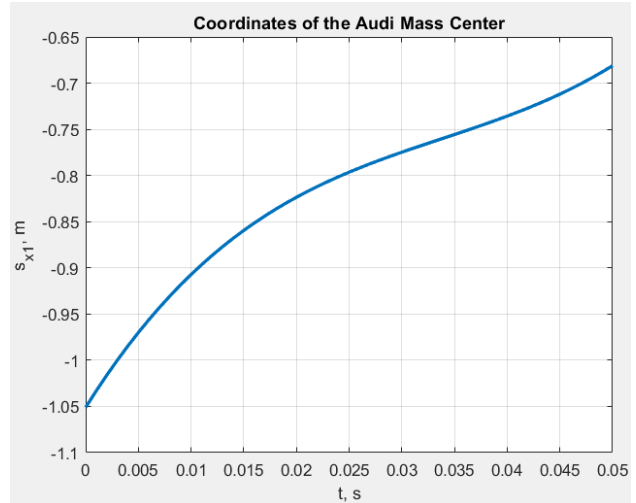**Fig.5**. Change in the velocity of the Audi center of mass in the impact phase.
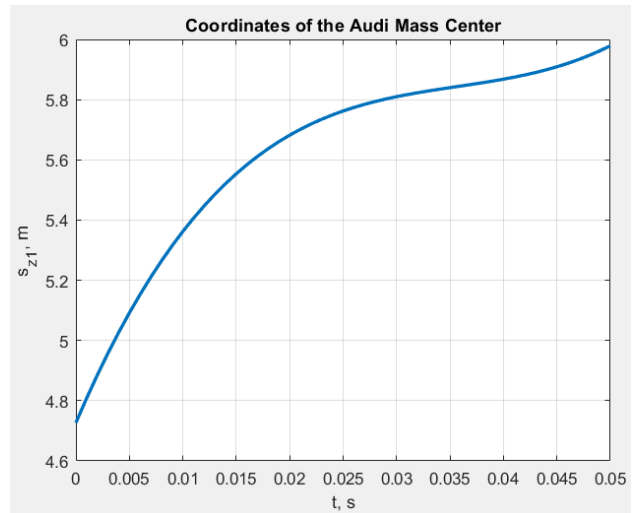
$$Z_1 = 2{,}044.10^4.t^3 - 2188.t^2 + 83{,}34.t + 4{,}727$$

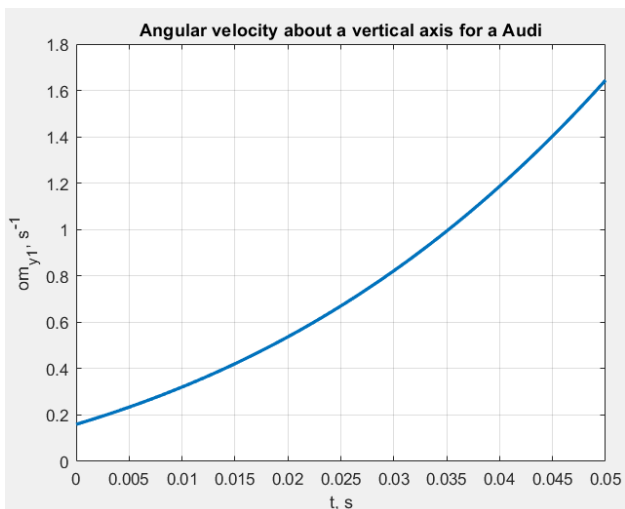**Fig.8**. Change of the Audi center-of-mass coordinates in the impact phase.

$$\dot{x}_1 = -1{,}223.10^4.t^3 + 317{,}8.t^2 - 52{,}8.t + 13{,}03$$

Fig.6. Change in the velocity of the Audi center of mass in the impact phase.

$$X_1 = 4199.t^3 - 426{,}4.t^2 + 18{,}22.t - 1{,}051$$

Fig.9. Change in the velocity of the Audi center-of-mass coordinates in the impact phase.

$$\omega_{y1} = 2038.t^3 + 217{,}6.t^2 + 13{,}71.t + 0{,}1597$$

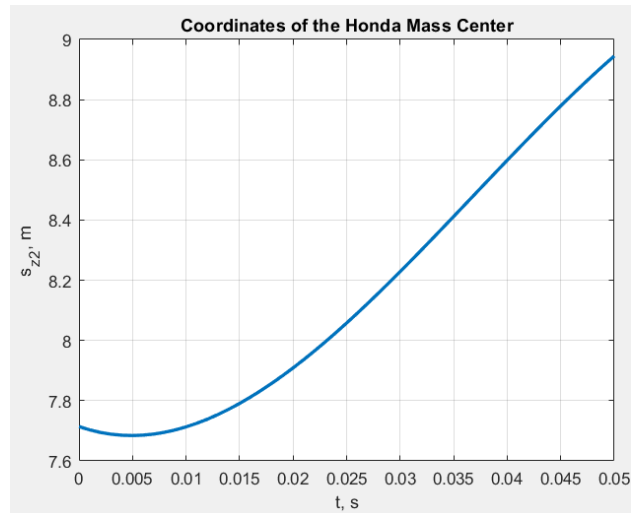**Fig. 7.** Change of the angular velocity about the vertical axis in the impact phase for an Audi.
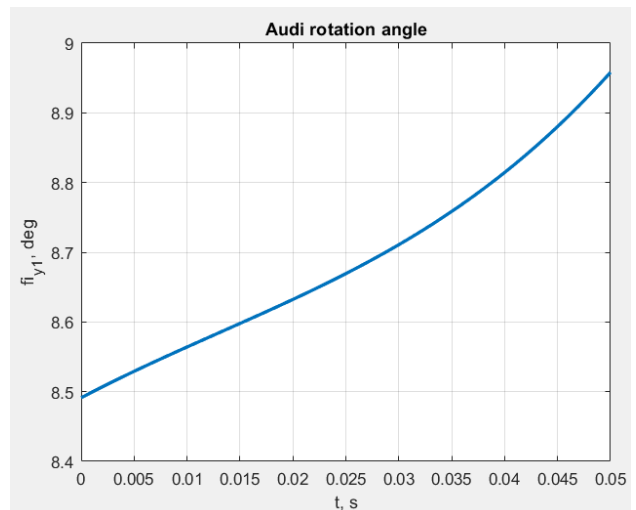
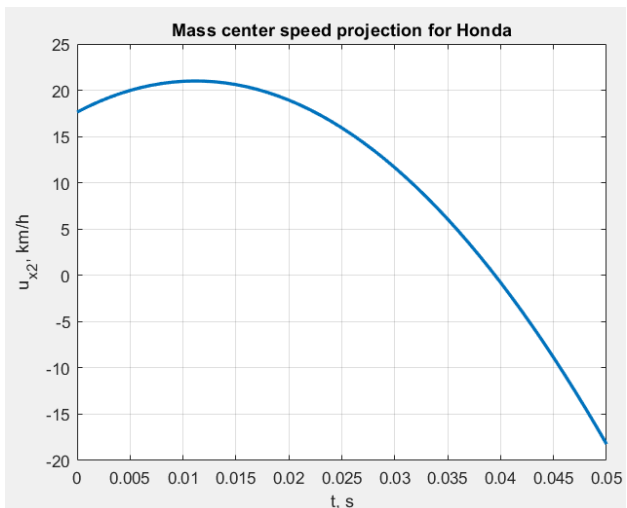$$\varphi_{y1} = 43{,}27.t^3 - 1{,}7.t^2 + 0{,}1398.t + 0{,}1482$$

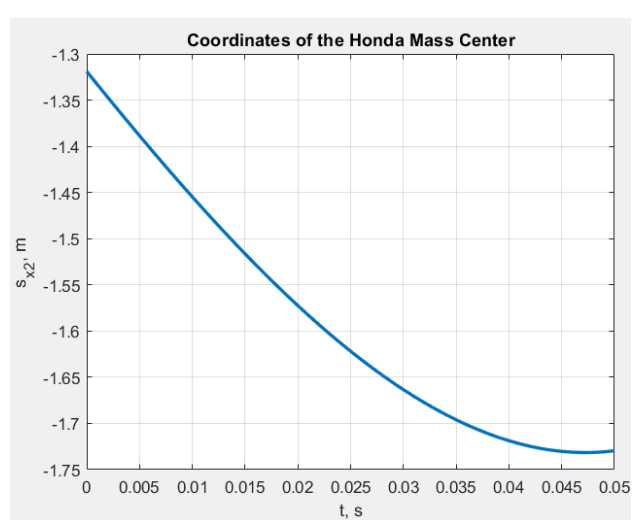**Fig.10.** Change in the angle of rotation of the Audi around the vertical axis.
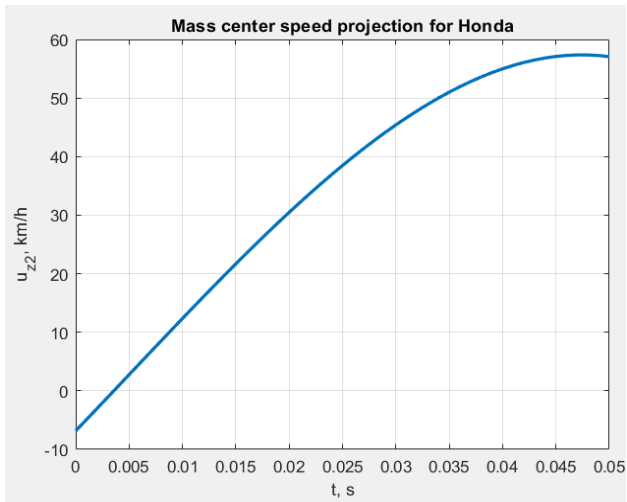
$$\dot{z}_2 = -3{,}588.10^5.t^3 + 5536.t^2 + 1898.t - 6{,}822$$

Fig.11. Change in the velocity of the Honda center of mass in the impact phase.

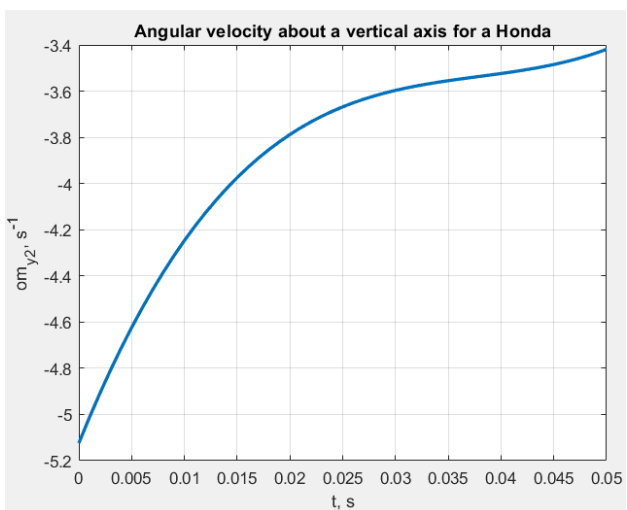$$\dot{x}_2 = 1{,}87.10^4.t^3 - 2{,}737.10^4.t^2 + 604{,}5.t + 7{,}64$$

Fig.12. Change in the velocity of the Honda center of mass in the impact phase.

$$\omega_{y2} = 2{,}498.10^4.t^3 - 2839.t^2 + 113{,}6.t - 5{,}124$$

Fig.13. Change of the angular velocity about the vertical axis in the impact phase for Honda.

$$Z_2 = -1{,}226.10^4.t^3 + 1354.t^2 - 12{,}43.t + 7{,}714$$

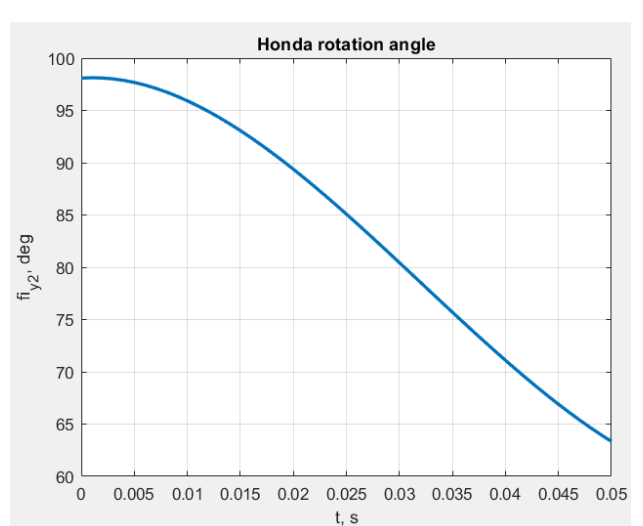**Fig.14.** Change of the Honda center-of-mass coordinates in the impact phase.

$$X_2 = 1469.t^3 + 45{,}9. - 14{,}18.t - 1{,}319$$

Fig.15. Change of the Honda center-of-mass coordinates in the impact phase.

$$\varphi_{y2} = 5773.t^3 - 555. + 1{,}187.t + 1{,}712$$

Fig.16. Change in the angle of rotation of the Honda around the vertical axis.

Therefore, the force of gravity $\vec{G}$ will lie on the axis Oz. The spatial arrangement model of the car is a plane located on four elastic supports, which are marked by $K_i(i = 1 \div 4)$ (Fig. 18).
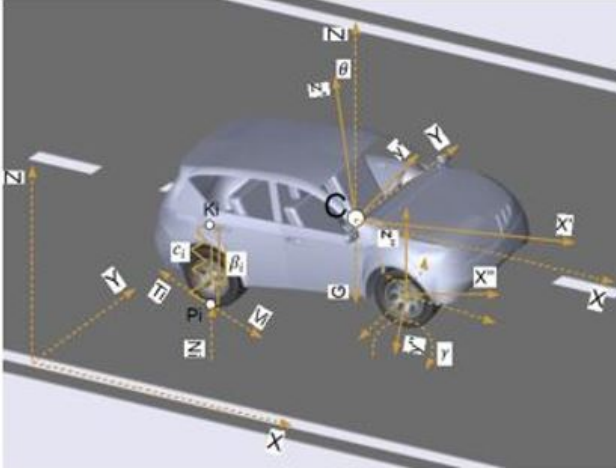

Fig. 17. Spatial dynamic model of an automobile with elastic suspension.

$\vec{F}_i(i = 1 \div 4)$ is elastic force generated by the elasticity of tires and springs; $\vec{N}_i(i = 1 \div 4)$ is normal reaction at the contact point of automobile tires, corresponding to elastic force; $\vec{V}_i(i = 1 \div 4)$ is velocity of the contact point P_i in the plane of the road Oxy; $\vec{T}_i(i = 1 \div 4)$ is friction force at the contact points that lies in the plane of the road Oxy; $\vec{R}_i(i = 1 \div 4)$ is resistance force generated by damping elements in suspension; $c_i, \frac{N}{m}(i = 1 \div 4)$ elasticity of suspension, taking into account both coefficient of elasticity

of tires and suspension; $b_i, \frac{N \cdot s}{m}(i = 1 \div 4)$ coefficient of linear resistance.

The car motion according to the studies of kinetic energy and generalized forces is defined by six differential equations with six generalized coordinates. These equations are valid if the friction force is in accordance with Coulomb's law and the wheels slide on the ground without rolling (Karapetkov [18, 19], Karapetkov, Uzunov [20]). According to (11), the wheels keep a continuous contact with the road.

Generalized forces and moments in the right-hand sides of the differential equations (8) are determined by assuming that the absolute coordinate system has a vertical axis of Oz.
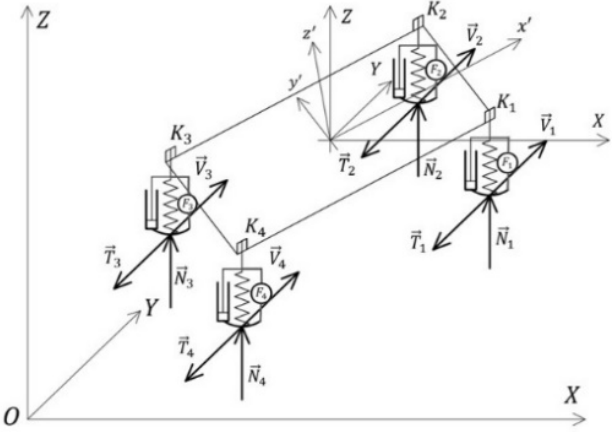

Fig. 18. Model of the forces acting on a car in its spatial motion, taking into account the elasticity of tires (suspension).

$$m \cdot \ddot{x} = \left[\sum_{i=1}^{4} F_{xi}\right]; \; m \cdot \ddot{y} = \left[\sum_{i=1}^{4} F_{yi}\right]; \; m \cdot \ddot{z} = \left[-G + \sum_{i=1}^{4} N_i - \sum_{i=1}^{4} R_i\right] \tag{7}$$

$$a_{11} \cdot \ddot{\varphi} + a_{12} \cdot \ddot{\psi} + a_{13} \cdot \ddot{\theta} =$$
$$\left\{ \begin{array}{c} \sum_{i=1}^{4} N_i \cdot \delta_{\varphi i} + \sum_{i=1}^{4} \left(F_{xi} \cdot f_{\varphi_{xi}} + F_{yi} \cdot f_{\varphi_{yi}}\right) - \sum_{i=1}^{4} R_i \cdot \delta_{\varphi i} \\ -b_{11} \cdot \dot{\varphi}^2 - b_{12} \cdot \dot{\psi}^2 - b_{13} \cdot \dot{\theta}^2 - c_{11} \cdot \dot{\varphi} \cdot \dot{\psi} - c_{12} \cdot \dot{\varphi} \cdot \dot{\theta} - c_{13} \cdot \dot{\psi} \cdot \dot{\theta} \end{array} \right\};$$

$$a_{21} \cdot \ddot{\varphi} + a_{22} \cdot \ddot{\psi} + a_{23} \cdot \ddot{\theta} =$$
$$= \left\{ \begin{array}{c} \sum_{i=1}^{4} \left(F_{xi} \cdot f_{\psi_{xi}} + F_{yi} \cdot f_{\psi_{yi}}\right) - b_{21} \cdot \dot{\varphi}^2 - b_{22} \cdot \dot{\psi}^2 - b_{23} \cdot \dot{\theta}^2 - \\ -c_{21} \cdot \dot{\varphi} \cdot \dot{\psi} - c_{22} \cdot \dot{\varphi} \cdot \dot{\theta} - c_{23} \cdot \dot{\psi} \cdot \dot{\theta} \end{array} \right\}; \tag{8}$$

$$a_{31} \cdot \ddot{\varphi} + a_{32} \cdot \ddot{\psi} + a_{33} \cdot \ddot{\theta} =$$
$$= \left\{ \begin{array}{c} \sum_{i=1}^{4} N_i \cdot \delta_{\theta i} + \sum_{i=i}^{4} \left(F_{xi} \cdot f_{\theta_{xi}} + F_{yi} \cdot f_{\theta_{yi}}\right) - \sum_{i=1}^{4} R_i \cdot \delta_{\theta i} - \\ -b_{31} \cdot \dot{\varphi}^2 - b_{32} \cdot \dot{\psi}^2 - b_{33} \cdot \dot{\theta}^2 - c_{31} \cdot \dot{\varphi} \cdot \dot{\psi} - c_{32} \cdot \dot{\varphi} \cdot \dot{\theta} - c_{33} \cdot \dot{\psi} \cdot \dot{\theta} \end{array} \right\};$$

$$a_{11} = J_{z'z'}; \; a_{12} = -J_{z'z'} \cdot cos\theta - J_{z'x'} \cdot sin\varphi \cdot sin\theta - J_{y'z'} \cdot cos\varphi \cdot sin\theta;$$

$$a_{13} = -J_{z'x'} \cdot cos\varphi + J_{y'z'} \cdot sin\varphi;$$

$$b_{11} = 0; \quad b_{12} = \begin{pmatrix} -\frac{1}{2} \cdot sin2\varphi \cdot sin^2\theta \cdot \left(J_{x'x'} + J_{y'y'}\right) + \\ + J_{x'y'} \cdot cos2\varphi \cdot sin^2\theta + \\ + \frac{1}{2} \cdot sin2\theta \cdot \left(J_{z'x'} \cdot cos\varphi - J_{y'z'} \cdot sin\varphi\right) \end{pmatrix};$$

$$b_{13} = \left(\frac{1}{2} \cdot \left(J_{x'x'} - J_{y'y'}\right) \cdot sin2\varphi - J_{x'y'} \cdot cos2\varphi\right);$$

$$c_{11} = 0; \quad c_{12} = 0; \quad c_{13} = \begin{pmatrix} cos2\varphi \cdot sin\theta \cdot \left(J_{x'x'} + J_{y'y'}\right) - \\ - J_{z'z'} \cdot sin\theta - \\ -2 \cdot \begin{pmatrix} J_{x'y'} \cdot sin2\varphi \cdot sin\theta + \\ + J_{z'x'} \cdot sin\varphi \cdot cos\theta + \\ + J_{y'z'} \cdot cos\varphi \cdot cos\theta \end{pmatrix} \end{pmatrix}$$

$$a_{21} = \left(J_{z'z'} \cdot cos\theta - J_{z'x'} \cdot sin\varphi \cdot sin\theta - J_{y'z'} \cdot cos\varphi \cdot sin\theta\right);$$

$$a_{22} = \begin{pmatrix} J_{x'x'} \cdot sin^2\varphi \cdot sin^2\theta + J_{y'y'} \cdot cos^2\varphi \cdot sin^2\theta + \\ + J_{z'z'} \cdot cos^2\theta - J_{x'y'} \cdot sin2\varphi \cdot sin^2\theta \\ - J_{x'z'} \cdot sin\varphi \cdot sin2\theta - J_{y'z'} \cdot cos\varphi \cdot sin2\theta \end{pmatrix};$$

$$a_{23} = \begin{pmatrix} 0.5 \cdot J_{x'x'} \cdot sin2\varphi \cdot sin\theta - \frac{1}{2} \cdot J_{y'y'} \cdot sin2\varphi \cdot sin\theta - \\ - J_{x'y'} \cdot cos2\varphi \cdot sin\theta - J_{z'x'} \cdot cos\varphi \cdot cos\theta + \\ + J_{y'z'} \cdot sin\varphi \cdot cos\theta \end{pmatrix};$$

$$b_{21} = \left(-J_{z'x'} \cdot cos\varphi + J_{y'z'} \cdot sin\varphi\right) \cdot sin\theta;$$

$$b_{22} = 0; \quad b_{23} = \begin{pmatrix} \begin{pmatrix} 0.5 \cdot J_{x'x'} \cdot sin2\varphi - \frac{1}{2} \cdot J_{y'y'} \cdot sin2\varphi - \\ - J_{x'y'} \cdot cos2\varphi \end{pmatrix} \cdot cos\theta + \\ + \left(J_{z'x'} \cdot cos\varphi - J_{y'z'} \cdot sin\varphi\right) \cdot sin\theta \end{pmatrix};$$

$$c_{21} = \begin{pmatrix} \left(J_{x'x'} \cdot sin2\varphi - J_{y'y'} \cdot sin2\varphi - 2 \cdot J_{x'y'} \cdot cos2\varphi\right) \cdot sin^2\theta - \\ - \left(J_{z'x'} \cdot cos\varphi - J_{y'z'} \cdot sin\varphi\right) \cdot sin2\theta \end{pmatrix};$$

$$c_{22} = \begin{pmatrix} \left(J_{x'x'} \cdot cos2\varphi - J_{y'y'} \cdot cos2\varphi + 2 \cdot J_{x'y'} \cdot sin2\varphi\right) \cdot sin\theta - \\ - J_{z'z'} \cdot sin\theta \end{pmatrix};$$

$$c_{23} = \begin{pmatrix} \left(J_{x'x'} \cdot sin^2\varphi + J_{y'y'} \cdot cos^2\varphi - J_{x'y'} \cdot sin2\varphi - J_{z'z'}\right) \cdot sin2\theta - \\ - 2 \cdot \left(J_{z'x'} \cdot sin\varphi + J_{y'z'} \cdot cos\varphi\right) \cdot cos2\theta \end{pmatrix};$$

$$a_{31} = J_{z'x'} \cdot cos\varphi + J_{y'z'} \cdot sin\varphi;$$

$$a_{32} = \begin{bmatrix} 0.5 \cdot \left(J_{x'x'} - J_{y'y'}\right) \cdot sin2\varphi \cdot sin\theta - J_{x'y'} \cdot cos2\varphi \cdot sin\theta - \\ - J_{z'x'} \cdot cos\varphi \cdot cos\theta + J_{y'z'} \cdot sin\varphi \cdot cos\theta \end{bmatrix};$$

$$a_{33} = J_{x'x'} \cdot cos^2\varphi + J_{y'y'} \cdot sin^2\varphi + \frac{1}{2} \cdot J_{x'y'} \cdot sin2\varphi; \quad b_{31} = J_{z'x'} \cdot sin\varphi + J_{y'z'} \cdot cos\varphi;$$

$$b_{32} = \begin{bmatrix} -\left[0.5 \cdot \begin{pmatrix} J_{x'x'} \cdot sin^2\varphi + J_{y'y'} \cdot cos^2\varphi + \\ + J_{z'z'} - J_{x'y'} \cdot sin2\varphi \end{pmatrix}\right] \cdot sin2\theta + \\ + \left(J_{z'x'} \cdot sin\varphi + J_{y'z'} \cdot cos\varphi\right) \cdot cos2\theta \end{bmatrix}; \quad b_{33} = 0;$$

$$c_{31} = \begin{bmatrix} \left[\left(J_{x'x'} + J_{y'y'}\right) \cdot cos2\varphi + 2 \cdot J_{x'y'} \cdot sin2\varphi + J_{z'z'}\right] \cdot sin\theta + \\ + 2 \cdot \left(J_{z'x'} \cdot sin\varphi + J_{y'z'} \cdot cos\varphi\right) \cdot cos\theta \end{bmatrix};$$

$$c_{32} = \left[\left(-J_{x'x'} + J_{y'y'}\right) \cdot sin2\varphi + 2 \cdot J_{x'y'} \cdot cos2\varphi\right]; \quad c_{33} = 0$$

We substitute the equations before $\delta_{\varphi i}$ and $\delta_{\theta i}$ using the notation

$$\delta_{\varphi i} = [(cos\varphi \cdot sin\theta) \cdot x'_{ki} + (-sin\varphi \cdot sin\theta) \cdot y'_{ki}];$$

$$\delta_{\theta i} = \begin{bmatrix} (sin\varphi \cdot cos\theta) \cdot x'_{ki} + \\ +(cos\varphi \cdot cos\theta) \cdot y'_{ki} + (-sin\theta) \cdot z'_{ki} \end{bmatrix}.$$

(9)

To facilitate notation, substitution has been done, which looks like as follows:

$$f_{\psi xi} = \begin{bmatrix} \begin{pmatrix} -sin\psi \cdot cos\varphi - \\ -cos\psi \cdot sin\varphi \cdot cos\theta \end{pmatrix} \cdot \delta x'_{ki} + \\ +\begin{pmatrix} sin\psi \cdot sin\varphi - \\ -cos\psi \cdot cos\varphi \cdot cos\theta \end{pmatrix} \cdot \delta y'_{ki} + \\ +(-cos\psi \cdot sin\theta) \cdot \delta z'_{ki} \end{bmatrix}; f_{\theta xi} = \begin{bmatrix} (sin\theta \cdot sin\psi \cdot sin\varphi) \cdot \delta x'_{ki} + \\ +(sin\theta \cdot sin\psi \cdot cos\varphi) \cdot \delta y'_{ki} + \\ +(-cos\theta \cdot sin\psi) \cdot \delta z'_{ki} \end{bmatrix}$$

$$f_{\varphi yi} = \begin{bmatrix} \begin{pmatrix} -sin\psi \cdot sin\varphi + \\ +cos\psi \cdot sin\varphi \cdot cos\theta \end{pmatrix} \cdot \delta x'_{ki} + \\ +\begin{pmatrix} -sin\psi \cdot cos\varphi - \\ -cos\psi \cdot sin\varphi \cdot cos\theta \end{pmatrix} \cdot \delta y'_{ki} \end{bmatrix}; f_{\psi yi} = \begin{bmatrix} \begin{pmatrix} cos\psi \cdot cos\varphi - \\ -sin\psi \cdot sin\varphi \cdot cos\theta \end{pmatrix} \cdot \delta x'_{ki} + \\ +\begin{pmatrix} -cos\psi \cdot sin\varphi - \\ -sin\psi \cdot cos\varphi \cdot cos\theta \end{pmatrix} \cdot \delta y'_{ki} + \\ +(sin\psi \cdot sin\theta) \cdot \delta z'_{ki} \end{bmatrix}$$

$$f_{\theta y} = \begin{bmatrix} (-cos\psi \cdot sin\varphi \cdot sin\theta) \cdot \delta x'_{ki} + \\ +(-cos\psi \cdot cos\varphi \cdot sin\theta) \cdot \delta y'_{ki} + \\ +(-cos\psi \cdot sin\theta) \cdot \delta z'_{ki} \end{bmatrix}$$

(10)

The relative motion of the wheels, the differential(s) and the engine are characterized by a system of four differential equations derived by the Lagrangian method, which has the form of

$$[I_\gamma] \cdot [\ddot{\gamma}] = [M_{\gamma i}];$$

$$M_{\gamma i} = \{F_{i\tau} \cdot r_i + sign\,(\dot{\gamma}_i) \cdot [M_{di} - f_i \cdot N_i - M_{si}]\}$$

$\vec{F}_{i\tau}$ is tangential component of the tire-road friction force, the positive direction of which is taken backwards, in the more frequent cases of braking or loss of stiffness.

Where μ is friction coefficient depending on slipping speed on the contact spot; $\vec{r}_i$ – radius of the wheel; f_i – coefficient of rolling friction; $\vec{N}_i$ – normal reaction of the road on wheels; $[I_\gamma]$ - a square matrix of coefficients in front the actual angular acceleration of the drive wheels, depending on the moment of inertia of the wheels and the engine; $\dot{\gamma}_i /i = 1 \div 4/$ - wheel angular velocity; $[\ddot{\gamma}]$ - a matrix-column of the actual angular acceleration of the wheels, two or four of which are propulsive; M_{di}, M_{si} - corresponding engine and brake torque applied to each wheel.

Figure 19 shows the dynamic model of an active suspension system. Figure 20 shows the dynamic diagram of a driving or sliding wheel.
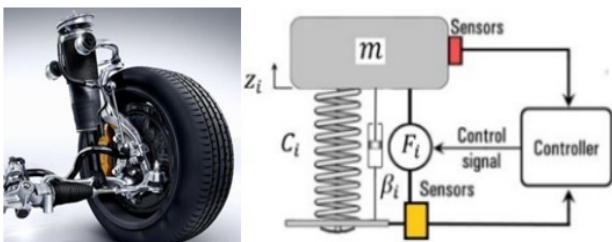

Fig. 19. Dynamic model of an active suspension system.

7. Results of the macro-movement of the cars after the impact

Initial conditions for the velocity of the center of mass and the angular velocity of the vehicle, satisfying the differential equations of motion, determine the residual energy of motion of the vehicles after impact. The graphs show the change of the kinematic parameters as a function of time (Fig. 21-29).
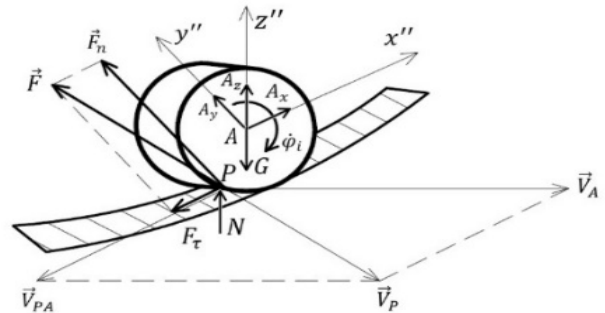
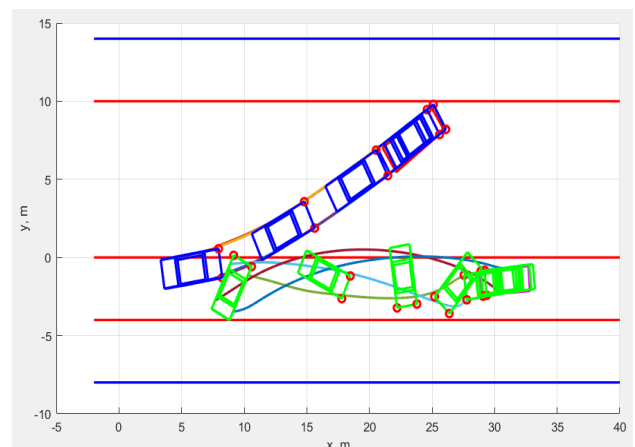(11)

Fig. 20. Drive wheel diagram.

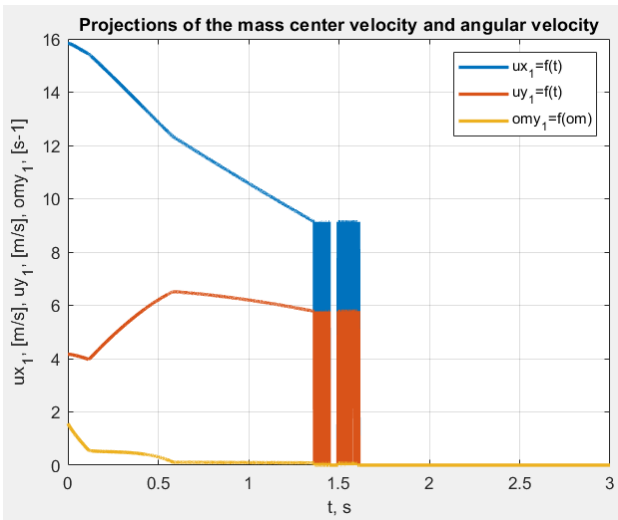**Fig. 21.** Motion of cars after the collision.

Fig.22. Change in the velocity of the Audi center of mass and angular velocity.
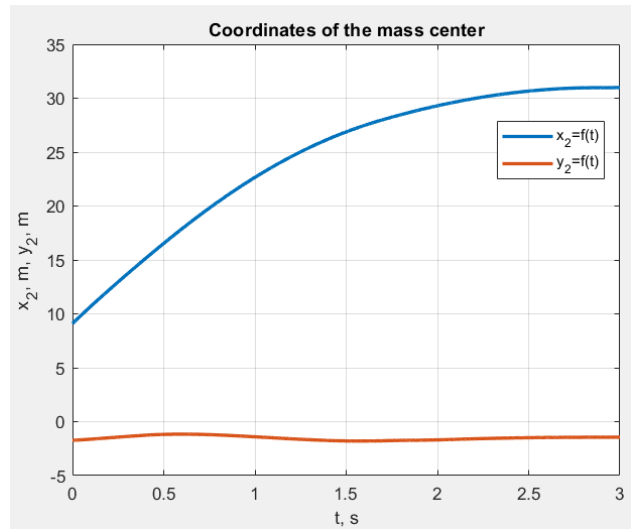

Fig.25. Change of the Honda center-of-mass coordinates.
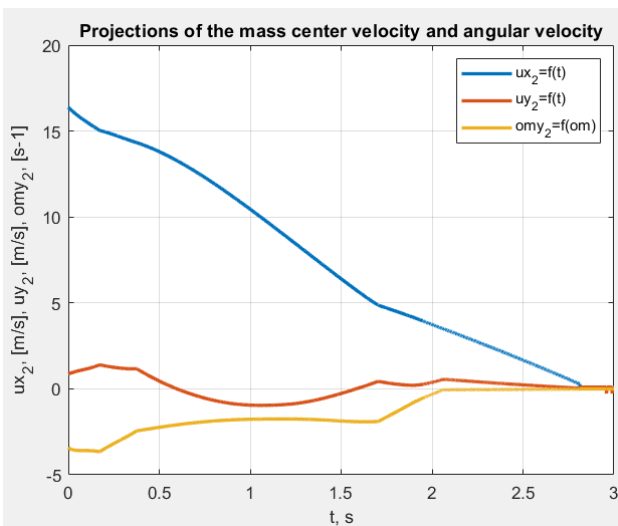

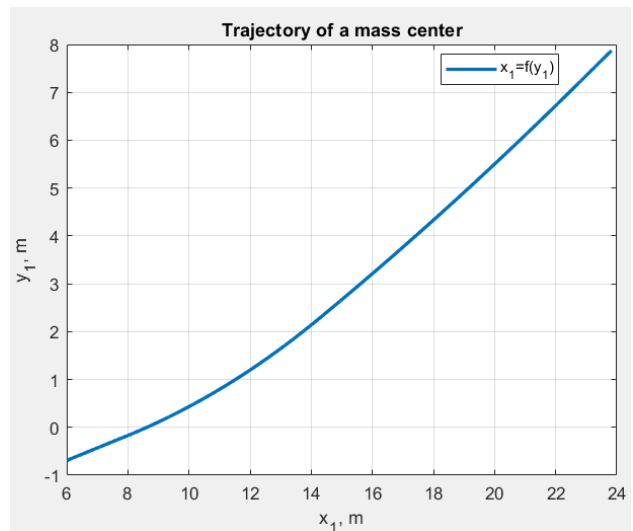**Fig.23.** Change in the velocity of the Honda center of mass and angular velocity.
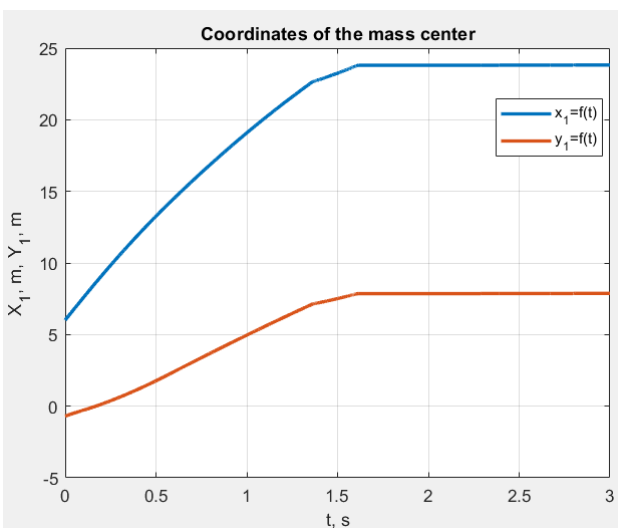

Fig.26. Audi center of mass trajectory.

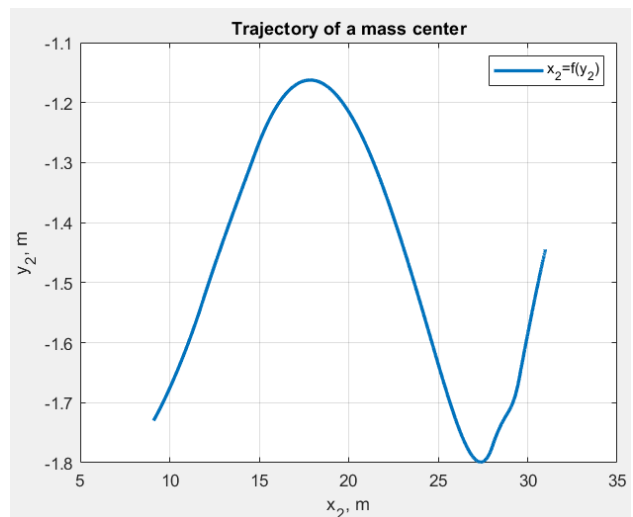**Fig.24.** Change of the Audi center-of-mass coordinates.

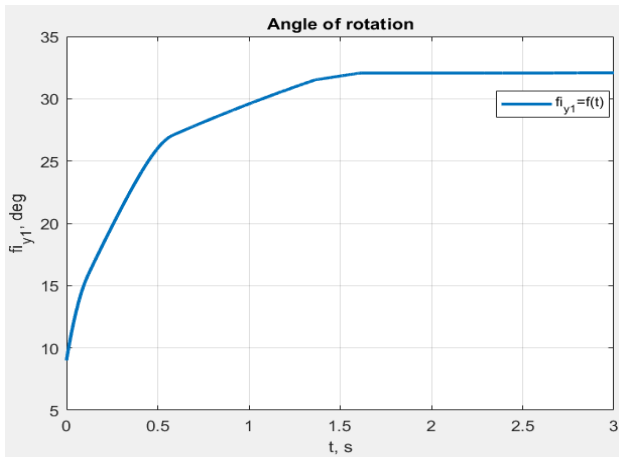**Fig.27.** Honda center of mass trajectory.

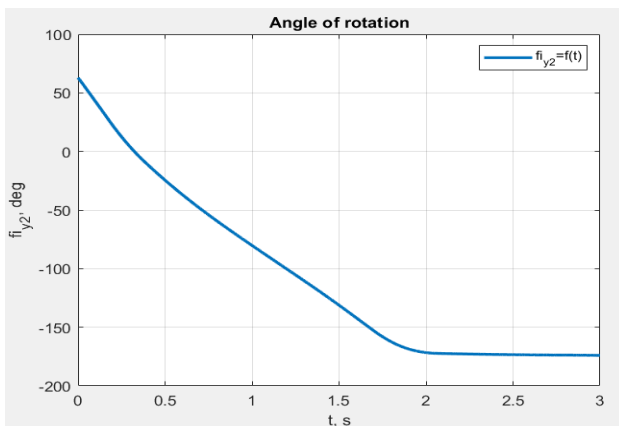**Fig.28.** Audi rotation angle about a vertical axis.

Fig.29. Honda rotation angle about a vertical axis.

8. Conclusions

1. A common engineering problem, known as the Cauchy problem, has been solved – the pre-impact velocity of the center of mass of automobiles using the finite element method has been determined. The traditional methods in this dynamic analysis, used in modern automotive expertise, do not meet the requirements for accuracy and precision.

2. The proposed finite element approach is a modern innovative tool for solving similar tasks in order to identify road accidents. In this way, the deformation zones can be reliably and reasonably analysed with sufficient accuracy.

3. The presented methodology for car impact can be offered for other vehicles, including service and freight vehicles - tractor trailers and semi-trailers. The solution of this problem requires corresponding adequate mechanical and mathematical modelling of vehicle motion after the impact.

References

1. Karapetkov, S., Dimitrov, L., Uzunov, H., Dechkova, S. Identifying Vehicle and Collision Impact by Applying the Principle of Conservation of Mechanical Energy. Transport and Telecommunication Riga, volume 20, no. 3, pp. 191–204, doi 10.2478/ttj-2019-0016, Latvia, (2019).
2. Karapetkov, S., Dimitrov, L., Uzunov, H., Dechkova, S. Examination of vehicle impact against stationary roadside objects. 9th International Scientific Conference on Research and Development of Mechanical Elements and Systems, IRMES 2019, University of Kragujevac, Faculty of EngineeringKragujevac; Serbia; 5 September 2019 through 7 September 2019; Code 154497, Kragujevac, Serbia, (2019).
3. Zlatev, Z., A. Ivanov. Development and Research of Information System Elements for Passengers Drive Comfort Improvement. Cybernetics and Information Technologies, 19(4), pp. 101–115, 2019.
4. Niehoff P., Gabler C., The Accuracy of WinSMASH Delta-V Estimates: The Influence of Vehicle Type, Stiffness, and Impact Mode. In the 50th Annual Proceedings of the Association for the Advancement of Automotive Medicine. Chicago, IL, 2006.
5. Wach W., Analiza deformacji samochodu według standardu CRASH3. Część 2: Pomiar głębokości odkształcenia (Analysis of motor vehicle deformation according to the CRASH3 standard. Part 2: Measurement of deformation depth). Paragraf na Drodze No. 12/2003.
6. SolidWorks Simulation 2009 – Training Manual, Dassault Systemes SolidWorksCorporation, Massachusetts, USA, 2009.
7. SolidWorks – Users Manual, Dassault Systemes SolidWorksCorporation, Massachusetts, USA, 2009.
8. Dechkova S., Creation of multi-mass models in the SolidWorks and Matlab environment for crash identification. Machine Mechanics №119, ISSN 0861-9727, pp. 28 – 32, Bulgaria 2018.
9. Nushtayev D.V. ABAQUS Posobiye dlya nachinayushchikh. Poshagovaya instruktsiya. SIMULA Moskva 2010
10. Yehia A. Abdel-Nasser. Frontal crash simulation of vehicles against lighting columns using FEM. Faculty of Engineering, Alexandria University. Production and hosting by Elsevier B.V. All rights reserved, doi.org/10.1016/j.aej.2013.01.005, 16 March 2013
11. Žmindáka, M., Z. Pelagića, P. Pastoreka, M. Močilana, M. Vybošťoka. Finite element modelling of high velocity impact on plate structures. The 20th International Conference: Machine Modeling and Simulations, MMS 2015
12. Duni, E., G. Monfrino, R. Saponaro, M. Caudano and F. Urbinati. Numerical simulation of full vehicle dynamic behaviour based on the interaction between abaqus/standard and explicit codes. ABAQUS Users' Conference, 2003.
13. Sharma D., Stern S., Brophy J., An Overview of NHTSA's Crash Reconstruction Software WinSMASH. In Proceedings of the Twentieth International Conference on Enhanced Safety of Vehicles, Paper No. 07-0211, Lyon, France, 2007.
14. Neptune J., Blair G., Flynn J., Amethod for quantifying vehicle crush stiffness coefficients," SAE Technical Paper Series, no. 920607, 1992.
15. Campbell K., Energy basis for collision severity, SAE Technical Paper Series, no. 740565, 1974.
16. Prasad K., CRASH3 Damage Algorithm Reformulation for Front and Rear Collisions. SAE 900098, 1990.
17. Prochowski L., Żuchowski A., Comparative Analysis of Frontal Zone of Deformation in Vehicles with SelfSupporting and Framed Bodies. Journal of KONES Powertrain and Transport, Vol. 18, No. 4, Warszawa, 2011.
18. Karapetkov, S. Auto Technical Expertise, Technical University - Sofia, Bulgaria (2005).
19. Karapetkov, S. Investigation of road traffic accident, technical commentary on the lawyer. Technical University of Sofia, Bulgaria, (2010).
20. Karapetkov, S., H. Uzunov. Dynamics of transverse resistance of a car. Didada Consult – Sofia, Bulgaria (2016).